

Design, synthesis and evaluation of acridin-9-yl hydrazide derivatives as BACE-1 inhibitors

Priti Jain^{1,2} · Pankaj K. Wadhwa¹ · Hemant R. Jadhav^{1,2}

Received: 18 November 2015 / Accepted: 11 April 2016
© Springer Science+Business Media New York 2016

Abstract BACE-1, an aspartyl protease is implicated in Alzheimer's disease. In this paper, we report BACE-1 inhibitory potential of acridin-9-yl hydrazide derivatives, known to inhibit other aspartyl proteases. The derivatives were designed based on the docking study, synthesized and assessed for BACE-1 inhibition in vitro. Docking simulation predicted the binding of prototype acridin-9-yl hydrazide at BACE-1 active site. The enzyme-inhibitor complex was primarily stabilized by hydrogen bonds between the hydrazide part of the inhibitor and side chain of Gly11, which is important amino acid of 10s loop. The acridinyl moiety showed π - π stacking with Tyr71 while the phenyl ring was buried in S1 cavity. Enzyme inhibition experiments showed that the synthesized compounds had moderate activity with compound **AA-13** having 54.54 % inhibition at 10 μ M concentration.

Keywords Acridin-9-yl hydrazides · BACE-1 inhibition · Alzheimer's disease · Docking study

Introduction

Aspartyl proteases are proteolytic enzymes belonging to the family of endonucleases. These are widely distributed and play important role in overall health and physiology (e.g., renin, chymosin, pepsin, napsin-A) as well as pathophysiology of various diseases. Their role is established in malaria (plasmepsins) (Azim *et al.*, 2008), AIDS (HIV protease) (Debouck, 1992), neoplastic disorders (cathepsin) (Fusek and Vetvicka, 1995) and neurodegenerative disorders (BACE-1 in Alzheimer's) (Jain and Jadhav, 2011).

Alzheimer's disease (AD) is a neurological disorder leading to memory loss and cognitive decline. So far, the drugs approved for AD, such as cholinesterase inhibitors (donepezil, rivastigmine, galantamine, tacrine) and NMDA receptor antagonist (memantine), are symptomatic and do not stop the progression of disease (Cumming, 1998). Hence, there are no drugs that stop or slow down the disease progression. Amyloid plaques and neurofibrillary tangles (NFTs) proposed in amyloid cascade hypothesis are the pathological hallmark for AD. As per this hypothesis, when amyloid precursor protein (APP) gets cleaved by secretases (β and γ) in a sequential fashion, it generates β -amyloid, i.e., A β -42, which is hydrophobic and fibrillogenic (Jain and Jadhav, 2013). It aggregates to form oligomers, accumulates in the brain and initiates a cascade of events that lead to neuronal dysfunctioning, neurodegeneration and neuronal fatality. Since, BACE-1 or β -secretase leads to the catalytic cleavage of APP, its inhibition can lead to reduction in A β -42 production (Suzuki *et al.*, 1994; Asami *et al.*, 1995; Shimizu *et al.*, 2008). BACE-1 knockout mice lacked A β expression and had no ill health effects (Asami *et al.*, 1995).

The 3D crystal structure of BACE-1 co-crystallized with different ligands reveals the basic requirements and the key

✉ Hemant R. Jadhav
hemantrj@pilani.bits-pilani.ac.in
Priti Jain
priti@pilani.bits-pilani.ac.in
Pankaj K. Wadhwa
pankaj.wadhwa@pilani.bits-pilani.ac.in

¹ Computational Chemistry Laboratory, Department of Pharmacy, Birla Institute of Technology and Science Pilani, Pilani Campus, Pilani, Rajasthan 333 031, India

² Medicinal Chemistry Laboratory, Department of Pharmacy, Birla Institute of Technology and Science Pilani, Pilani Campus, Pilani, Rajasthan 333 031, India

features needed for enzyme inhibition. BACE-1 has a catalytic aspartate dyad and three hydrophobic pockets S1, S2' and S3. The inhibitor must have: (1) a group that acts as H-bond donor to form H-bonding interactions with catalytic Asp228 and Asp32, (2) hydrophobic groups to occupy S1 cavity (formed by the side chains of Tyr71, Phe108, Trp115, Ile118 and Leu30) and S3 (formed by side chains of Trp115 and Ile110, as well as main chains of Gln12, Gly11, Gly230, Thr231, Thr232 and Ser35), (3) polar groups to bind in S2' cavity having Ile126, Trp76, Val69, Arg128, Tyr198 amino acid residues (Jain *et al.*, 2016).

Azim *et al.* have reported acridinyl hydrazides as potent inhibitors of cathepsin-D and plasmepsin-II (Azim *et al.*, 2008). However, inhibition of BACE-1 by these compounds is hitherto not been studied. Hence, in this study, we have tried to explore acridin-9-yl hydrazide derivatives as BACE-1 inhibitors for the treatment of Alzheimer's disease.

Design

In the last decade, several drug discovery strategies have been exploited in search of BACE-1 inhibitors. The inhibitors with therapeutic potential would require, besides good potency and pharmacokinetic properties, low molecular weight (<500 daltons) and high lipophilicity in order to penetrate the blood–brain barrier. Keeping this in mind and knowing that acridine derivatives are reported to inhibit aspartyl proteases, we attempted to design acridin-9-yl hydrazide derivatives for BACE-1 inhibition.

Compound **AA-11** (Fig. 1) was conceived as prototype and was docked in BACE-1 protein (PDB id: 2OHP). It was observed that the enzyme–inhibitor complex was primarily stabilized by hydrogen bonds between the hydrazide part of

the inhibitor and Asp32. The acridinyl moiety showed π – π stacking with Tyr71, occupied the S2' region while the phenyl ring was buried in S1 cavity. It showed significant interactions, accommodation of substrate-binding clefts and a good docking score which was better than the standard ligand 6IP-389. Based on these observations, a library of derivatives with various electron-donating and electron-withdrawing substituents was synthesized (Scheme 1) to study the effect of substituents on BACE-1 inhibition.

Materials and methods

General

Reaction progress was monitored by TLC using precoated silica gel G plates (Keisegel 60F254, Merck) and visualized using UV light. Melting points were measured with Buchi 530 melting point apparatus and were uncorrected. ^1H NMR spectra were recorded on a Bruker Avance 400 MHz system using DMSO as solvent. Chemical shifts (δ) are reported in parts per millions (ppm) relative to TMS as internal standard. FTIR spectra were performed on IR Prestige 21 Shimadzu using KBr as standard. Mass spectra were recorded on Waters Acquity instrument in electrospray mode. Unless otherwise stated, all reagents were obtained from commercial suppliers and used without further purification. Compounds were named as per ChemDraw Ultra 11.0 software.

General procedure for the synthesis of 9-hydrazinyl acridine (1)

9-aminoacridine was dissolved in concentrated hydrochloric acid (HCl) and cooled to about 0 °C. Cooled solution of

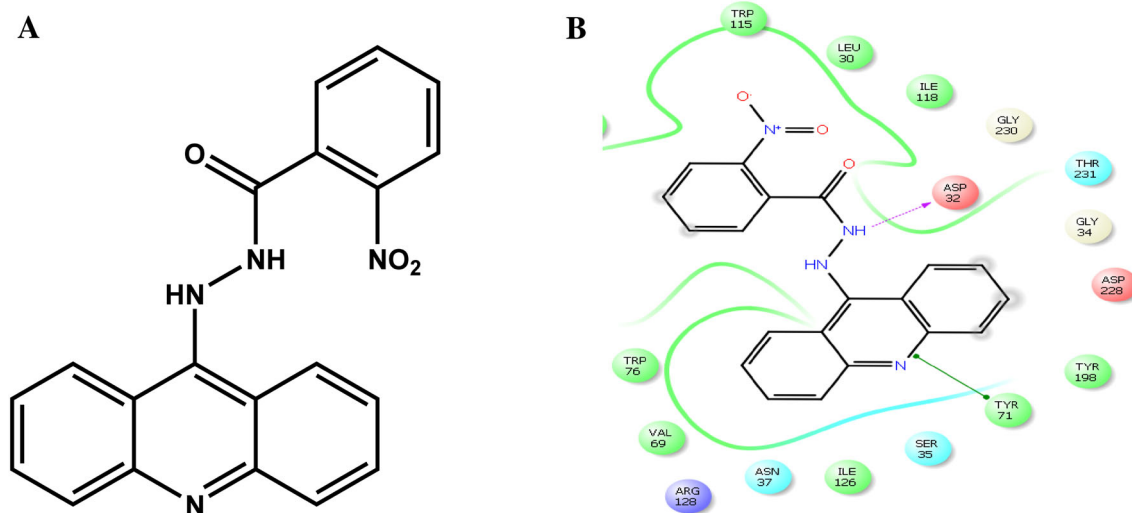
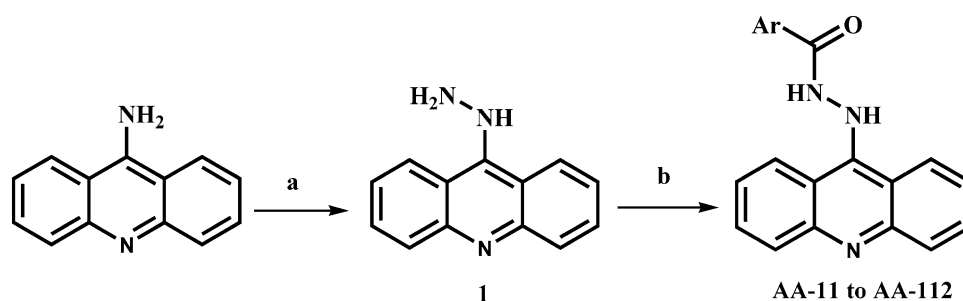


Fig. 1 a Chemical structure of AA-11, b 2D interaction plot of AA-11

Scheme 1 Reagents and conditions: *a* NaNO₂, HCl, -5 to 0 °C, 1 h; SnCl₂, HCl, *b* HOBT, EDC HCl, THF, TEA, substituted carboxylic acids, 0 °C, 12 h



sodium nitrite in water (1.1 equivalent) was slowly added to the above maintaining temperature at about 0 °C for about 1 h till the reaction was over. To the diazotized product, acidified stannous chloride was slowly added till completion of the reaction. The reduced product was then worked up with sodium hydroxide (NaOH) and extracted with ethyl acetate. The solvent was distilled under reduced pressure, and crude compound was crystallized to get pure 9-hydrazinyl acridine.

General procedure for the synthesis of substituted benzoic acid *N'*-acridin-9-yl hydrazide (AA-11 to AA-112)

1.5 equivalents of substituted carboxylic acid was added to tetrahydrofuran (THF) and allowed to stir till complete dissolution. To it was added 1.5 equivalent of hydroxy-*O*-benzotriazole (HOBT) and *N*-(3-dimethylaminopropyl)-*N'*-ethylcarbodiimide-HCl (EDC-HCl) and stirred for 15–20 min at ice-cold condition. To this solution were added triethylamine (TEA) and 1.5 equivalent of 9-hydrazinyl acridine. The reaction was run at ice-cold condition till completion and worked up with dichloromethane (DCM), washed with dil HCl and sodium bicarbonate (NaHCO₃). DCM layer was collected, and solvent was evaporated under reduced pressure. The final solid product was crystallized. The characterization details are given below:

9-Hydrazinyl acridine (**1**) IR (cm⁻¹): 3410.58 (sec. N–H stretching), 3319.49 (sec. N–H stretching), 3217.31 (Aromatic C–H stretching), 2864.29 (Aliphatic C–H stretching), 1716.65 (C=O), 1587.42–1438.90 (Aromatic C=C stretch); ¹H NMR (400 MHz, DMSO, δppm): 1.91 (s, –NH₂), 3.60 (br, 1H, –NH), 7.27 (dd, 2H, Ar–H), 7.60 (dd, 2H, Ar–H), 7.82 (d, 2H, Ar–H), 8.37 (d, 2H, Ar–H).

N'-(Acridin-9-yl)-2-nitrobenzohydrazide (**AA-11**) Yield: 59.74 %, mp 279 °C, IR (cm⁻¹): 3331.07 (sec. N–H stretching), 3275.13 (Amide N–H stretch), 1641.42 (C=O stretching), 1588.42–1504.48 (Aromatic C=C stretch), ¹H NMR (400 MHz, DMSO, δppm): 4.11 (s, 1H, –NH), 7.02–8.10 (m, 13H, 12Ar–H and 1 –NH).

N'-(Acridin-9-yl)-3-fluorobenzohydrazide (**AA-12**) Yield: 72.42 %, mp 290 °C, IR (cm⁻¹): 3390.49 (sec. N–H stretching), 3235.14 (Amide N–H stretch), 1631.78 (C=O stretching), 1588.42–1516.07 (Aromatic C=C stretch), ¹H NMR (400 MHz, DMSO, δppm): 4.18 (s, 1H, –NH), 7.22–8.02 (m, 13H, 12Ar–H and 1 –NH).

N'-(Acridin-9-yl)-2-fluorobenzohydrazide (**AA-13**) Yield: 80.40 %, mp 270 °C, IR (cm⁻¹): 3275.13 (Amide N–H stretch), 3028.24 (Aromatic C–H stretching), 1680.00 (C=O stretching), 1641.42–1504.48 (Aromatic C=C stretch), ¹H NMR (400 MHz, DMSO, δppm): 4.09 (s, 1H, –NH), 7.15–8.06 (m, 13H, 12Ar–H and 1 –NH).

N'-(Acridin-9-yl)-4-fluorobenzohydrazide (**AA-14**) Yield: 52.35 %, mp 310 °C, IR (cm⁻¹): 3361.49 (sec. N–H stretching), 3292.31 (Amide N–H stretch), 3097.68 (Aromatic C–H stretching), 1692.65 (C=O stretching), 1587.42–1438.90 (Aromatic C=C stretch), ¹H NMR (400 MHz, DMSO, δppm): 4.06 (s, 1H, –NH), 7.11–8.10 (m, 13H, 12Ar–H and 1 –NH).

N'-(Acridin-9-yl)-4-chlorobenzohydrazide (**AA-15**) Yield: 79.89 %, mp 298 °C, IR (cm⁻¹): 3415.93 (sec. N–H stretching), 1651.07 (C=O stretching), 1562.65–1497.01 (Aromatic C=C stretch), ¹H NMR (400 MHz, DMSO, δppm): 4.06 (s, 1H, –NH), 7.15–8.18 (m, 13H, 12Ar–H and 1 –NH).

N'-(Acridin-9-yl)-2-bromobenzohydrazide (**AA-16**) Yield: 68.97 %, mp 277 °C, IR (cm⁻¹): 3361.49 (sec. N–H stretching), 3292.31 (Amide N–H stretch), 3097.68 (Aromatic C–H stretching), 1692.65 (C=O stretching), 1587.42–1438.90 (Aromatic C=C stretch); ¹H NMR (400 MHz, DMSO, δppm): 3.63 (br, 1H, –NH), 7.09–8.58 (m, 13H, 12 Ar–H and 1 –NH).

N'-(Acridin-9-yl)-2,4-dichlorobenzohydrazide (**AA-17**) Yield: 76.29 %, mp 288 °C, IR (cm⁻¹): 3372.20 (sec. N–H stretching), 3102–3010 (Aromatic C–H stretching), 1648.27 (C=O stretching), 1525.06–1412.64 (Aromatic C=C stretch), ¹H NMR (400 MHz, DMSO, δppm): 4.15 (s, 1H, –NH), 7.42–8.15 (m, 12H, 11Ar–H and 1 –NH).

N'-(4-(2-(Acridin-9-yl)hydrazinecarbonyl)phenyl)acetamide (**AA-18**) Yield: 68.92 %, mp 285 °C, IR (cm⁻¹): 3356.14 (sec. N–H stretching), 3251.98 (Amide N–H stretch), 1645.28 (C=O), 1588.42–1427.42 (Aromatic C=C stretch), ¹H NMR (400 MHz, DMSO, δppm): 2.04 (s, 3H, –CH₃), 4.10 (s, 1H, –NH), 7.46–8.12 (m, 14H, 12Ar–H and 2 –NH).

N'-(Acridin-9-yl)-3-methoxybenzohydrazide (**AA-19**) Yield: 65.40 %, mp 285 °C, IR (cm⁻¹): 3390.49 (sec. N–H stretching), 3235.55 (Amide N–H stretch), 3040–3018 (Aromatic C–H stretching), 2894 (Aliphatic C–H stretching), 1621.45 (C=O stretching), 1582.42–1518.05 (Aromatic C=C stretch), ¹H NMR (400 MHz, DMSO, δppm): 3.86 (s, 3H, OCH₃), 4.13 (s, 1H, –NH), 6.95–8.28 (m, 13H, 12 Ar–H and 1 –NH).

N'-(Acridin-9-yl)-3,4-dimethoxybenzohydrazide (**AA-110**) Yield: 83.26 %, mp 286 °C, IR (cm⁻¹): 3390.49 (sec. N–H stretching), 3277.06 (Amide N–H stretch), 1639.49 (C=O stretching), 1591.27–1516.05 (Aromatic C=C stretch), ¹H NMR (400 MHz, DMSO, δppm): 3.73–3.78 (s, 6H, 2OCH₃), 4.15 (s, 1H, –NH), 6.84–8.12 (m, 12H, 11Ar–H and 1 –NH).

N'-(Acridin-9-yl)-3-amino-4-methylbenzohydrazide (**AA-111**) Yield: 57.24 %, mp 275 °C, IR (cm⁻¹): 3334.92 (sec. N–H stretching), 2925 (Aliphatic C–H stretching), 1639.49 (C=O stretching), 1586.39–1516.30 (Aromatic C=C stretch), ¹H NMR (400 MHz, DMSO, δppm): 2.35 (s, 3H, –CH₃), 4.05–4.61 (hump, 3H), 6.99–7.98 (m, 12H, 11 Ar–H and 1 –NH).

N'-(Acridin-9-yl)isonicotinohydrazide (**AA-112**) Yield: 74.57 %, mp 301 °C, IR (cm⁻¹): 3277.06 (Amide N–H stretch), 3026.31 (Aromatic C–H stretch), 1641.42 (C=O stretching), 1565.42–1504.05 (Aromatic C=C stretch), ¹H NMR (400 MHz, DMSO, δppm): 3.98 (s, 1H, –NH), 7.42–9.06 (m, 13H, 12Ar–H and 1 –NH).

In vitro evaluations

BACE-1 in vitro assay was carried out using fluorescence resonance energy transfer (FRET) technique. The BACE-1 FRET assay kit was purchased from Pan Vera, Life Technologies (kit no P2985, Madison, WI, USA), and the assay was carried out according to the protocol provided by the supplier. The measure of inhibitory activity of compounds is based upon the reduction in the fluorescence quantum yield due to inhibition of BACE-1 enzymatic activity. The protease substrate (APP-based peptide) consists of a fluorescence donor (rhodamine) connected to a quenching acceptor through a peptide sequence (EVNLDAEFK). The fluorescence is weak intrinsically due to resonance energy transfer, but upon enzymatic cleavage, the quantum yield of donor molecule increases. Inhibitory potential of the designed

compounds can be governed from the reduced fluorescence quantum yield. The assay was conducted in 50 mM sodium acetate buffer (pH 4.5) using 3X BACE-1 enzyme (1U/ml). The screening of test compounds was performed at 10 μM concentration. The test compounds were diluted with DMSO to prepare the stock solution of 10 mM and further diluted with buffer to achieve desired concentration of 10 μM. The incubation time was kept 60 min following which the fluorescence was read on Tecan multiwell spectrofluorometer (excitation: 545 nm; emission: 590 nm). Oral bioavailability prediction was done using JChem for Excel. It helps in identifying the compounds with good oral bioavailability and also CNS penetration; the crucial parameter needed for the design of BACE-1 inhibitors.

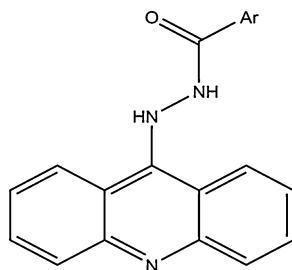
Docking simulation and in silico physicochemical properties prediction

X-ray crystal structure of human BACE-1 (pdb code—2OHP) in complex with aminopyridine derivative was retrieved from Brookhaven protein database for docking study. It was prepared for missing charges, missing bonds and flexibility. Its model was then constructed through grid generation on Maestro by removing all the water molecules. Ligands were prepared using LigPrep module of Schrodinger Suite 2013. All possible ionization states at pH 7.0 ± 2.0 were enumerated using Epik and minimized. Docking simulations were performed using Glide (Friesner *et al.*, 2004). Validation of docking protocol was done to govern the reliability and reproducibility of the docking parameters used for the study. The docking strategy revealed that the docked ligand superimposed well with the reference ligands (co-crystallized ligand) with RMSD value of 0.385 Å.

Oral bioavailability of the synthesized compounds was predicted using JChem for Excel, and blood–brain barrier (BBB) was predicted using online BBB permeation predictor software available at <http://www.cbligand.org/BBB/>. These data help in identifying the compounds with good oral bioavailability and central nervous system (CNS) penetration; the crucial parameter needed for the design of BACE-1 inhibitors. It is proposed that reducing the peptidic nature molecular weight and logP, along with polar surface area (PSA), could result in highly potent BACE-1 inhibitor with enhanced brain permeation. The physicochemical properties for the synthesized compounds are shown in Table 1.

Results and discussion

Total of 12 acridin-9-yl hydrazide derivatives having electron-donating as well as electron-withdrawing groups were synthesized. Synthesized derivatives were tested for

Table 1 Physicochemical properties and in vitro data of Acridin-9-yl hydrazide derivatives

Code	-Ar	Glide score	MW	HBA	HBD	PSA	LogP	BBB score	% Inhibition ^a
AA-11	<i>o</i> -NO ₂ -Ph	-4.48	358.10	5	2	98.41	4.39	0.041	41.80
AA-12	<i>m</i> -F-Ph	-6.73	331.12	3	2	55.27	4.60	0.091	34.54
AA-13	<i>o</i> -F-Ph	-5.85	331.11	3	2	55.27	4.60	0.070	24.18
AA-14	<i>p</i> -F-Ph	-5.64	331.11	3	2	55.27	4.60	0.090	27.90
AA-15	<i>p</i> -Cl-Ph	-5.92	347.08	3	2	55.27	5.06	0.080	32.18
AA-16	<i>o</i> -Br-Ph	-6.45	391.03	3	2	55.27	5.22	0.080	31.45
AA-17	(<i>o,p</i> -di-Cl)-Ph	-6.90	381.04	3	2	55.27	5.66	0.062	32.00
AA-18	(<i>p</i> -NHCOCH ₃)-Ph	-7.95	370.14	4	3	84.37	3.69	0.097	52.72
AA-19	<i>m</i> -OCH ₃ -Ph	-5.68	343.38	4	2	64.5	4.30	0.065	43.54
AA-110	(<i>m,p</i> -di-OCH ₃)-Ph	-6.31	373.14	5	2	73.73	4.14	0.022	53.27
AA-111	(<i>m</i> -NH ₂ , <i>p</i> -CH ₃)-Ph	-7.96	342.14	4	3	81.29	4.14	0.070	54.45
AA-112	-C ₅ H ₄ N (Isonicotinic acid)	-5.68	314.11	4	2	68.16	3.24	0.094	37.18

MW molecular weight, HBA hydrogen bond acceptor, HBD hydrogen bond donor, PSA polar surface area

^a % Inhibition at 10 μM concentration, values are mean of triplicate experiments performed independently

BACE-1 inhibition at 10 μM concentration, docking was performed using Glide (Schrodinger suite), and the docking scores and % BACE-1 inhibition values are given in Table 1. Overall, the acridin-9-yl hydrazide derivatives displayed consistent BACE-1 inhibition profile. Visual analysis of docking poses (Fig. 2) was done to correlate with % inhibition values. The docking studies revealed occupance of substrate-binding cavities and interactions with active site amino acids.

It was observed that compound AA-12 substituted with *m*-fluoro group on the phenyl ring displayed interaction with Asp32. The acridine nitrogen formed hydrogen bond with the main chain of Gly230. Acridine ring had π-π stacking with Trp115 covering the S2' cavity and phenyl ring occupied the S1 pocket. Placing the fluoro group at *ortho* and *para* position (AA-13, AA-14) further affected the activity negatively. Compound AA-12 showed 34.54 % inhibition while AA-13 and AA-14 had 24.18 % and 27.90 % inhibition, respectively. The in vitro results were supported by docking study where AA-12 scored higher than AA-13 and AA-14. It was observed that placing an *o*-fluoro or *p*-fluoro group (AA-13, AA-14) instead of *m*-fluoro diminished the aspartate interactions though AA-13

formed key interaction with 10s loop amino acid Gly11. As compared to other deactivating groups like nitro (AA-11) and bromo (AA-16) at *ortho* position, fluorine was found to be least active. This can be explained from docking study whereby it is observed that fluorine being highly electronegative gets solvent exposed, changing the conformation in such a way that interaction of amide nitrogen with Asp32 does not occur. Since this is not the case with bromine- and nitro-substituted compounds, these compounds show interaction with Asp32. Placing *o,p*-dichloro (compound AA-17) promoted interactions with Asp32, Tyr71, placed the acridine ring in S2' cavity while phenyl ring occupied S1 pocket and had better docking score as compared to other electron-withdrawing substituted derivatives. However, it did not show any advantage in % inhibition studies.

Comparatively, compound AA-18 having *p*-acetamido substitution formed contacts with Asp32, showed π-π stacking with Tyr71 and Phe108 and had 52.72 % BACE-1 inhibition. Compound AA-19 bearing *m*-methoxy substitution indicated that the enzyme-inhibitor complex was primarily stabilized by hydrogen bonds between the hydrazide part of the inhibitor and side chain of Gly11,

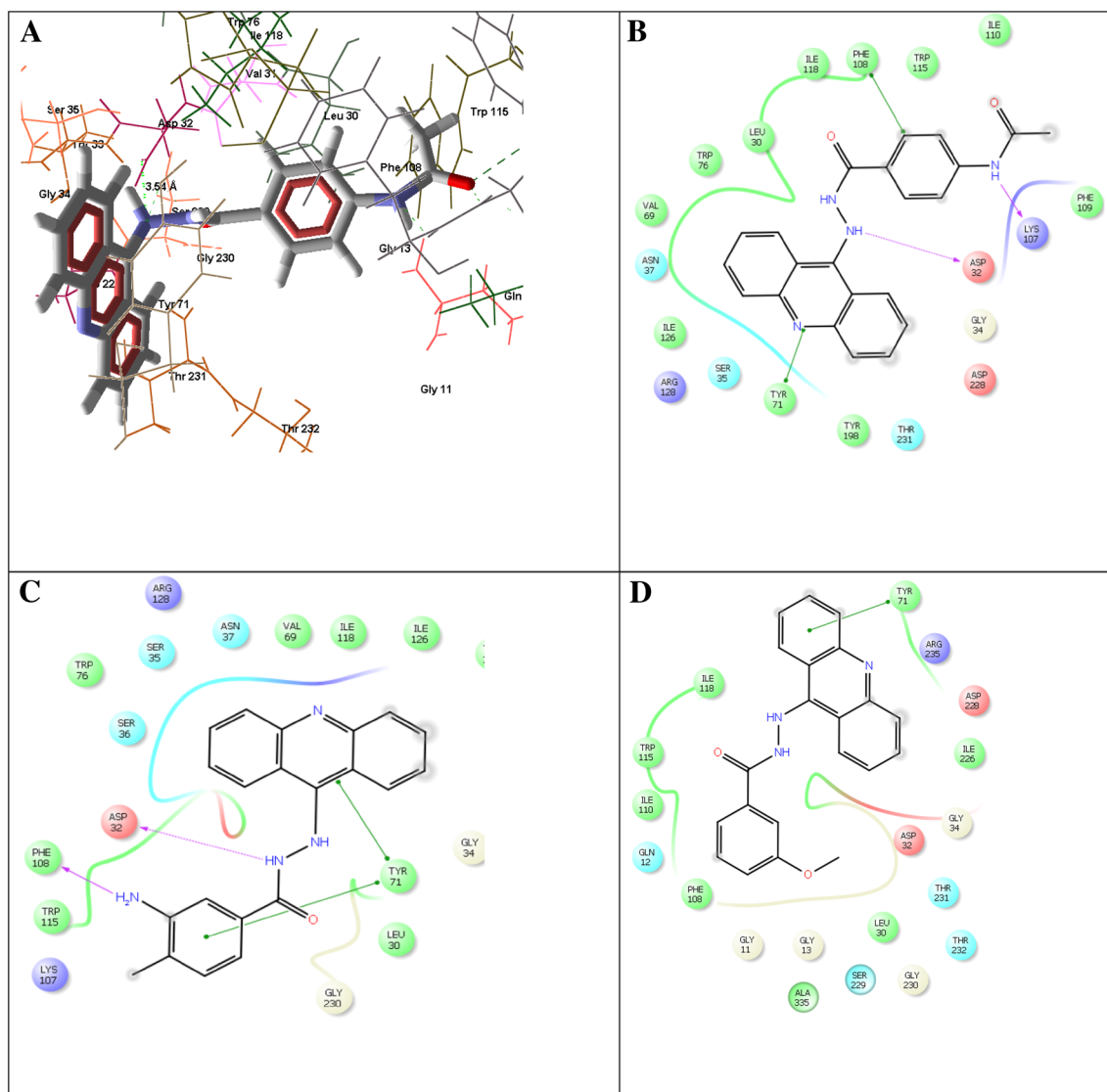


Fig. 2 Docking poses of few Acridin-9-yl hydrazide derivatives. **a** Docked pose of AA-18, **b** 2D interaction plot of AA 18, **c** 2D interaction plot of AA-111, **d** 2D interaction plot of AA-19

which is important amino acid of 10s loop. The acridinyl moiety showed π - π stacking with Tyr71 while the phenyl ring was buried in S1 cavity. It failed to interact with the aspartate dyad nevertheless. **AA-110** with *m,p*-dimethoxy phenyl group also showed similar interactions viz: hydrogen bonding interaction with Asp32, amine group of phenyl ring formed interaction with Phe108 and π - π stacking of both the rings with Tyr71. However, it showed 53.27 % BACE-1 inhibition in vitro. Most active compound **AA-111**, having *m*-amino and *p*-methyl phenyl group, showed that NH of hydrazine formed hydrogen bonding interaction with Asp32, amine group of phenyl ring formed interaction with Phe108 and π - π stacking of both the rings with Tyr71. The electron-donating substitution appears to increase the potency, but it also makes the compounds polar and may

reduce brain permeation. Both, **AA-18** and **AA-111**, displayed highest docking score in the series, and this result was concurrent with BACE-1 inhibition (52.72 and 54.54 %, respectively).

It was observed that replacing benzoyl on hydrazine with isonicotinoyl, as in compound **AA-112**, reduced the interactions as well as BACE-1 inhibition.

Considering in vitro–in silico results and to substantiate their lead-like nature, in silico prediction of oral bioavailability and BBB permeation was made. The log *p* values for all derivatives were within range of 3.24–5.66, hydrogen bond donor count between 2 and 3 and hydrogen bond acceptor count from 3 to 5. It is reported that BBB permeability is affected by polar surface area (PSA), and PSA should be below 90 Å² for CNS active agents (Pajouhesh

and Lenz, 2005). Except **AA-11**, all compounds had polar surface area less than or near to 70 \AA^2 and, hence, BBB permeability for the series was predicted to be good. Further, using online BBB permeation prediction software, BBB permeability was predicted, wherein any compound having SVM_MACCSFP BBB score of more than 0.02 will be able to cross BBB. It was found that all the compounds had score above 0.02 and hence were predicted to cross BBB. All these parameters indicate that these derivatives will have good oral bioavailability and will cross blood–brain barrier.

Conclusion

Acridin-9-yl hydrazide derivatives, reported to inhibit other aspartyl proteases, were explored as BACE-1 inhibitors. As indicated by docking scores as well as in vitro BACE-1 inhibition, it was observed that electron-donating substitution on benzoyl moiety is preferred over electron-withdrawing substituents. All the compounds showed occupancy of S1 and S2' cavity and except compounds **AA-13** and **AA-19**, and all derivatives had interaction with Asp32, which is essential for activity. The designed derivatives were also predicted to be orally bioavailable and BBB penetrant. Further modification with respect to inclusion of groups to enhance binding with catalytic aspartate dyad (Asp32 and Asp228) and substitution of electron-donating groups on benzoyl moiety may lead to enhanced binding and potency.

Compliance with ethical standards

Conflict of interest The authors confirm that this article content has no conflict of interest.

References

- Asami OA, Ishibashi Y, Kikuchi T, Kitada C, Suzuki N (1995) Long amyloid β protein secreted from wild type human neuroblastoma IMR-32 cells. *Biochemistry* 34:10272–10278
- Azim MK, Ahmed W, Ishtiaq AK, Nosheen AR, Khalid MK (2008) Identification of acridinyl hydrazides as potent aspartic protease inhibitors. *Bioorg Med Chem Lett* 18:3011–3015
- Cumming JL (1998) Alzheimer's disease: etiologies, pathophysiology, cognitive reserve and treatment opportunities. *Neurology* 51:512–517
- Debouck C (1992) The HIV-1 protease as a therapeutic target for AIDS. *AIDS Res Hum Retroviruses* 8:153–164
- Friesner RA, Banks JL, Murphy RB, Halgren TA, Klicic JJ, Mainz DT, Repasky MP, Knoll EH, Shelley M, Perry JK, Shaw DE, Francis P, Shenkin PS (2004) Glide: a new approach for rapid, accurate docking and scoring. 1. Method and assessment of docking accuracy. *J Med Chem* 47:1739–1749
- Fusek M, Vetvicka V (1995) Aspartic Proteinases Physiology and Pathology. CRC Press, Boca Raton
- Jain P, Jadhav HR (2011) Therapeutic advances in the treatment of Alzheimer's disease: present and future. *Curr Drug Ther* 6:175–185
- Jain P, Jadhav HR (2013) Quantitative structure activity relationship analysis of aminoimidazoles as BACE-I inhibitors. *Med Chem Res* 22:1740–1746
- Jain P, Wadhwa PK, Rohilla S, Jadhav HR (2016) Rational design, synthesis and in vitro evaluation of allylidene hydrazinecarboximidamide derivatives as BACE-1 inhibitors. *Bioorg Med Chem Lett* 26:33–37
- Pajouhesh H, Lenz GR (2005) Medicinal chemical properties of successful central nervous system drugs. *NeuroRx* 2:541–553
- Shimizu H, Tosaki A, Kaneko K, Hisano H, Sakurai T, Nukina N (2008) Crystal structure of an active form of BACE-I, an enzyme responsible for amyloid protein production. *Mol Cell Biol* 28:3663–3671
- Suzuki N, Cheung TT, Cai XD, Odaka A, Otvos L, Eckman C, Golde TE, Younkin SG (1994) An increased percentage of long amyloid β protein secreted by familial amyloid β -protein precursor (β APP717) mutants. *Science* 264:1336–1340